

Structural, Dielectric and Magnetolectric Effect in Piezomagnetic-Piezoelectric Composites

Muaamar Abdulazeez Kamil

Department of Physics, University of Tikrit, Al-Qadissiya, P.O. Box 42, Tikrit, Sallahaldin, Iraq

Abstract: Magnetolectric composites of $(x) \text{Ni}_{0.5} \text{Zn}_{0.5} \text{Fe}_2\text{O}_4$ [NZFO]+(1-x) PLZT in which x varies as 0, 0.15, 0.30 and 1 were prepared by solid-state reaction technique. The presence of single phase in $x = 0$ and $x = 1$ as well as two phases in $x = 0.15, 0.30$ and 0.45 composites was confirmed by X-Ray Diffraction (XRD) technique. Scanning electron microscopy was employed for micro-structural studied. The variation of dielectric constant (ϵ') with frequency (100-5 MHz) has been also studied. The static Magnetolectric (ME) voltage coefficient was measured as function of applied DC magnetic field and variation in ME response has been explained in terms of the contents of piezomagnetic phase and intensity of applied magnetic field. The maximum ME conversion factor of 6.26 mV/cm.Oe was observed for 15% NZFO+85% PLZT composite.

Key words: Magnetolectric effect, piezoelectric composites, composites material, XRD, solid state

INTRODUCTION

Bulk magnetolectric composites consisting of ferrimagnetic and ferroelectric phases could be used for device application such as data storage, switching, modulation of amplitudes, polarization and filters, waveguides, transducers and spin wave generation, etc. (Rivera and Schmid, 1991; Mori and Wuttig, 2002; Nan *et al.*, 2003; Zhao *et al.*, 2005). These materials exhibiting simultaneously long range electric and magnetic ordering stimulates an intense search for a new substance with similar properties (Broutman and Krock, 1967a, b). However, a selection of suitable combination of ferroelectric phase and ferrite phase material with a view to achieve ME effect itself is a challenging task. The reasons being: the ferrite phase is required to have high piezomagnetic coefficient and its resistivity must be comparable to that of the ferroelectric phase: the piezoelectric coefficient of ferroelectric phase should also high and its resistivity should be at least of the order of $10^{12} \Omega\text{-cm}$ and the mechanical coupling between ferrite and ferroelectric phase must be perfect (Patankar *et al.*, 2001). Following this principle, various ME bulk composites have been prepared such as $\text{Ni}(\text{Co}, \text{Mn}) \text{Fe}_2\text{O}_4\text{-BaTiO}_3$, $\text{CoFe}_2\text{O}_4\text{-BaTiO}_3$, $\text{NiFe}_2\text{O}_4\text{-BaTiO}_3$, $\text{NiFe}_2\text{O}_4\text{-Pb}_{0.93}\text{La}_{0.07}(\text{Zr}_{0.60}\text{Ti}_{0.40})\text{O}_3$ ($\text{Ni}, \text{Co})\text{Fe}_2\text{O}_4\text{-}[0.67 \text{Pb}(\text{Mg}_{1/3}\text{Nb}_{2/3})\text{O}_3\text{-}0.33 \text{PbTiO}_3]$ (Koops, 1951; Van Run *et al.*, 1974; Van Den Boomgaard *et al.*, 1976; Suryanarayana, 1994; Mahajan *et al.*, 2000; Sheikh and Mathe, 2009; Fawzi *et al.*, 2010). Therefore, in the present work, we report on synthesis of NZFO, PLZT and $(x) \text{NZFO}+(1-x) \text{PLZT}$ composites where $x = 0.15, 0.30$ and 0.45 by

solid-state reaction technique. The sum properties of the composites such as dielectric properties are studied in order to understand the conduction mechanism in composite. Ferroelectric and magnetic properties of composites were studied with change content of individual phases of composites.

MATERIALS AND METHODS

Experimental details: The NZFO was synthesized by using conventional solid-state reaction technique where NiO , ZnO and Fe_2O_3 were used as initial ingredients. These oxides were mixed and milled for 3 h and presintered at 900°C for 12 h. Presintered NZFO was milled again and finally calcined at 1200°C for 12 h. PLZT was prepared by solid-state reaction technique. The starting materials were analytical reagent grade oxides, viz. PbO , La_2O_3 , ZrO_2 and TiO_2 . These oxides were mixed in the proper molar proportions, milled for 3 h and presintered at 800°C for 4 h. Finally the material was calcined in a closed crucible at 1100°C for 12 h and slowly cooled to room temperature in the furnace.

NZFO phase and PLZT phase were identified using X-Ray Diffraction (XRD) technique. These calcined phases were milled for 3-4 h after mixing in the required molar proportions (i.e., 15, 30 and 45% NZFO phase with 85, 70 and 55% PLZT phase, respectively) and pressed in a die to form pellets of 2 mm thick and 10 mm in diameter using a hydraulic press pump. Final sintering of the constituent phases and their composites was carried out at 1150°C for 10 h and cooled slowly in the furnace. The crystal structure of the calcined powders was analyzed

using X-ray diffraction technique (model Bruker D8 Advance). The static ME voltage coefficient (i.e., DC $(dE/dH)_H$) was measured using Keithley Electrometer (Model 6514) in DC magnetic field using the same set up. The experimental arrangement of ME output is similar to that used previously (Kanamadi *et al.*, 2005).

RESULTS AND DISCUSSION

Figure 1 is shows X-Ray Diffraction (XRD) patterns of individual phases NZFO, PLZT and composites $x = 0.15, 0.30$ and 0.45 . The composites with $x = 0.15, 0.30$ and 0.45 are designated as A, B and C, respectively. All diffraction peaks in the XRD patterns of NZFO and PLZT were indexed using JCPDS data for Ni-Zn ferrite and PLZT (7/60/40) (Card Nos. 8-234 and 46-0504) which revealed a cubic spinel structure for NZFO and tetragonal perovskite structure for PLZT samples. All diffraction peaks in XRD pattern of all composites are assigned to either NZFO or PLZT. There is no unidentified diffraction peak indicating absence of intermediate phase of any un-reacted phase even after sintering composites at 1150°C . The individual phases have not reacted with each other. The relative intensity of X-ray diffraction peaks depend on the relative abundance of the particular phases in composites. The X-ray diffraction patterns of composites reveal that the intensity as well as number of NZFO peaks increase with increasing NZFO content in composites. These results are in agreement with literature (Patankar *et al.*, 2001). The lattice parameters of the pure NZFO phase: $a = 8.41 \text{ \AA}$ and pure PLZT phase: $a = 4.0815 \text{ \AA}, c =$

4.0845 \AA and $c/a = 1.0007$, respectively. The lattice strain and average crystallite size were calculated using Hall equation (Haertling, 1999):

$$\frac{\beta \cos \theta}{\lambda} = \frac{1}{\epsilon} + \frac{\eta \sin \theta}{\lambda} \tag{1}$$

Where:

- ϵ = Effective crystallite size
- η = Effective strain
- β = Full Width at Half Maximum (FWHM) lattice for NZFO and PLZT phases (Gorter 1954) of the diffraction peak
- λ = X-ray wavelength
- θ = Bragg diffraction angle

The curve $\beta \cos \theta / \lambda$ versus $\sin \theta / \lambda$ shows approximately a linear variation as seen in Fig. 2a and b. The effective crystallite size and strain are calculated using a linear equation: $y = \eta x + 1/\epsilon$, the slope of these lines given strain while their intercept on y-axis shows the effective crystallite size. The negative slope for indicates the presence of the Scanning Electron Microscopy (SEM) micrographs of all composites are shown in Fig. 3a-c. A typical SEM image shows the two different phases distinctly, i.e., gray for PLZT and dark for NZFO, indicating that NZFO and PLZT are randomly mixed together. NZFO and PLZT phases are uniformly distributed as seen. The connectivity of ferrite grains is broken by the distribution of nonmagnetic PLZT grains which may lead to variations of magnetic properties of the composite (Viswanathan and Murthy, 1990).

Figure 4 shows the variation of dielectric constant as a function of frequency for the composites at room

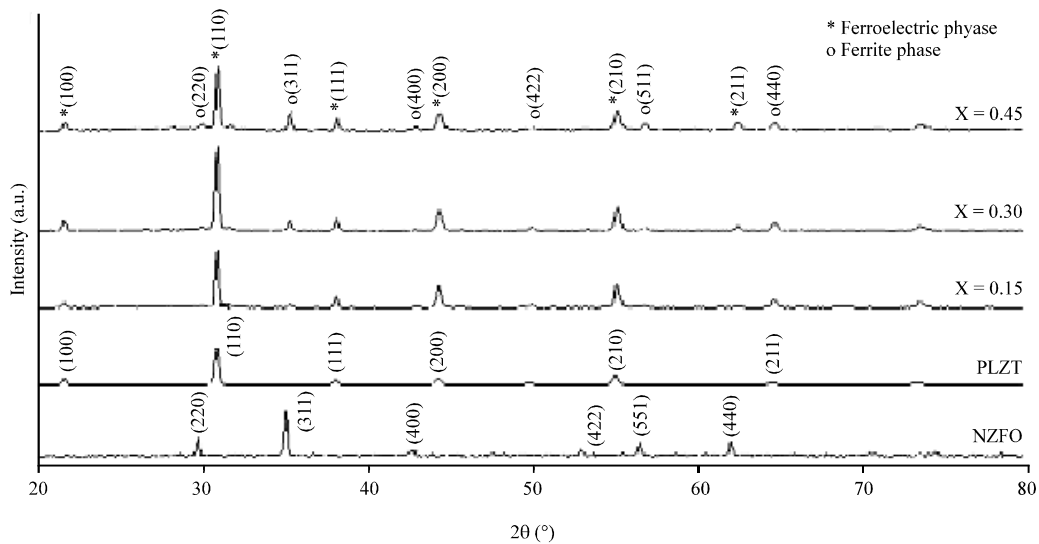


Fig. 1: X-ray diffraction pattern of NZFO phase, PLZT phase and their composites

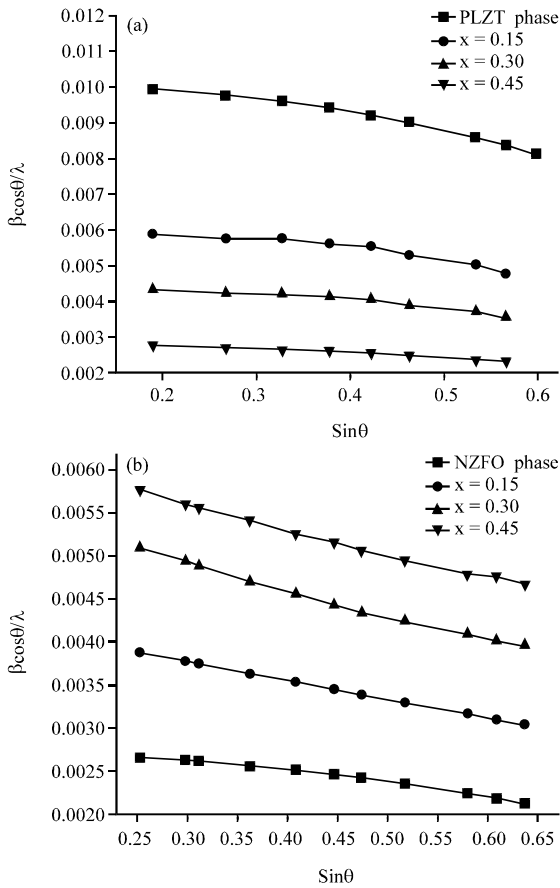


Fig. 2: Compositional dependent lattice strain for: a) PLZT and b) NZFO phase present in ME composites effective compressive strain in the crystal

temperature. The dielectric constant decreases rapidly with increase in frequency, shows dispersion in the lower frequency region and attains a saturation limit at higher frequencies. The all composites show dispersion due to Maxwell-Wagner type interfacial polarization in agreement with the phenomenological theory by Koops (1951). The pattern at lower frequencies may be attributed to different types of polarizations (electronic, atomic, interfacial, ionic, etc). The high value of the dielectric constant observed at low frequencies is explained on the basis of space charge polarization due to inhomogeneous dielectric structure. The inhomogeneities in the present system are impurities, porosity and grain structure (Kanamadi *et al.*, 2005). At higher frequencies dielectric constant remains independent of frequency due to inability of electric dipoles to follow the alternating applied electric field (Patankar *et al.*, 2001). These frequency independent values are known as static values of dielectric constant.

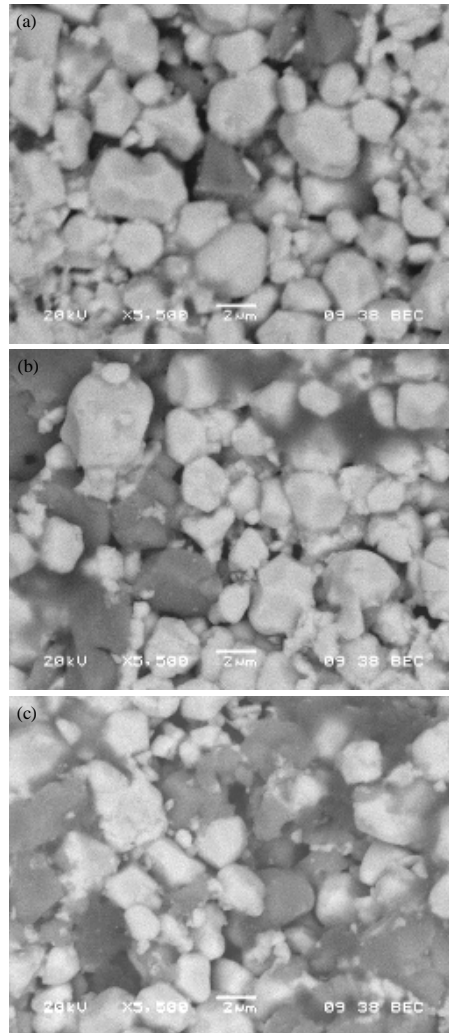


Fig. 3: SEM micrographs of (x) NZFO+(1-x) PLZT composites with: a) x = 0.15; b) x = 0.30 and c) x = 0.45

Figure 5 shows the typical dependence of the ME conversion on DC magnetic field for composites (x) $Ni_{0.5}Zn_{0.5}Fe_2O_4+(1-x)$ PLZT under study. The magnetic bias dependence of dE/dH was similar for all three composites. As evidenced from the figure, the ME voltage coefficient increases with increasing magnetic bias, saturating at a bias level of ~ 1200 Oe. This saturation field corresponds to the field at which saturation magnetization is reached in $Ni_{0.5}Zn_{0.5}Fe_2O_4$. For all composites the highest ME value was obtained for 1200 Oe, DC field indicating that the magnetostrictive phase has reached a saturation value producing constant electric field in the piezoelectric phase, hence making dE/dH decrease with increasing magnetic field. This indicates that magnetic saturation occurs at low

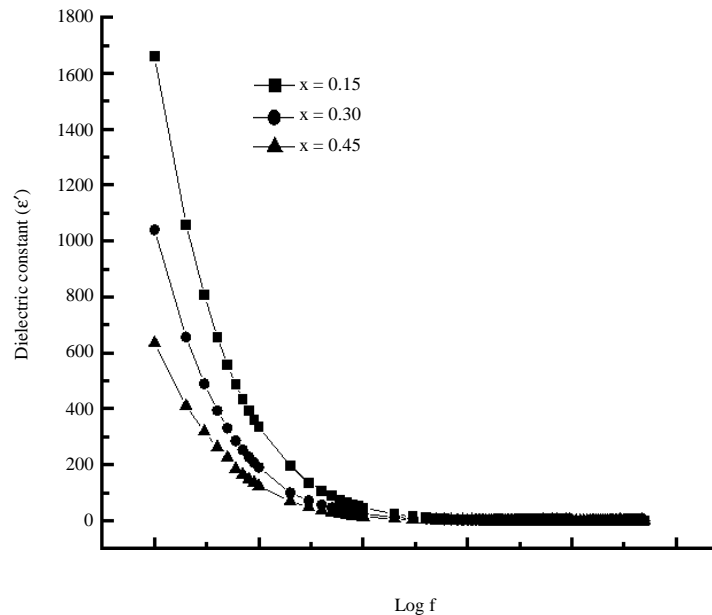


Fig. 4: Variation of dielectric constant (ϵ') with frequency for $x = 0.15, 0.30$ and 0.45 composites

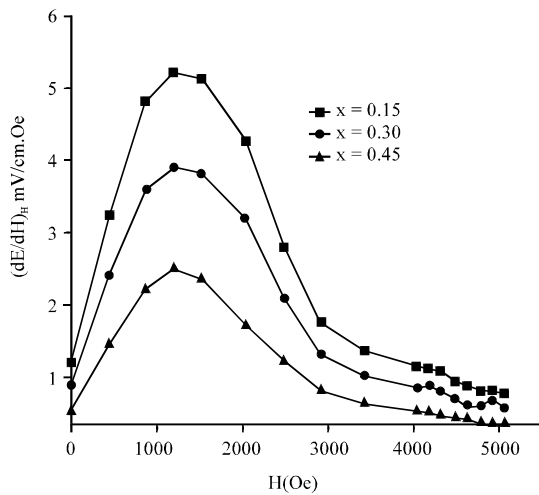


Fig. 5: Variation of ME voltage coefficient with applied magnetic field for (x) NZFO+ $(1-x)$ PLZT composites

stimulation and the samples are best suited in responding to relatively weak magnetic field. The behavior of the magnetic field dependence of ME voltage coefficient is similar to that for the magnetostrictive behavior (Van Den Boomgaard *et al.*, 1976; Nan *et al.*, 2003).

CONCLUSION

The present composites prepared by solid state reaction have only ferrite phase (NZFO) and ferroelectric phase (PLZT) in them without any impurity or

intermediate phase. The strain calculations using Hall equation show a negative slope for both the phases in ME composites indicating the presence of tensile strain. Dielectric constant with frequency shows dispersion in all composites. The variation of magnetoelectric voltage coefficient with applied fields suggests its dependence on the molar percentage of constituent phases. A maximum ME coefficient of 6.26 mV/cm.Oe has been observed in the composite with 15% NZFO+85% PLZT composite.

REFERENCES

Broutman, L.J. and R.H. Krock, 1967a. Electrical conduction and magnetoelectric effect in $\text{CuFe}_{1.8}\text{Cr}_{0.2}\text{O}_4\text{-Ba}_{0.8}\text{Pb}_{0.2}\text{TiO}_3$ composites. *J. Electroceram.*, 6: 115-122.

Broutman, L.J. and R.H. Krock, 1967b. *Modern Composite Materials*. Addison Wesley Publishing Co., London, UK.

Fawzi, A.S., A.D. Sheikh and V.L. Mathe, 2010. Multiferroic properties of Ni ferrite-PLZT composites. *Physica B: Condens. Matter*, 405: 340-344.

Gorter, E.W., 1954. Saturation magnetization and crystal chemistry of ferrimagnetic oxides. *Philips Res. Rep.*, 9: 321-355.

Haertling, G.H., 1999. Ferroelectric ceramics: History and technology. *J. Am. Ceramic Soc.*, 82: 797-818.

Kanamadi, C.M., L.B. Pujari and B.K. Chougule, 2005. Dielectric behaviour and magnetoelectric effect in $(x) \text{Ni}_{0.8}\text{Cu}_{0.2}\text{Fe}_2\text{O}_4+(1-x)\text{Ba}_{0.9}\text{Pb}_{0.1}\text{Ti}_{0.9}\text{Zr}_{0.1}\text{O}_3$ ME composites. *J. Magn. Magnet. Mater.*, 295: 139-144.

- Koops, C.G., 1951. On the dispersion of resistivity and dielectric constant of some semiconductors at audiofrequencies. Phys. Rev., Vol. 83. 10.1103/PhysRev.83.121.
- Mahajan, R.P., K.K. Patankar, N.M. Burange, S.C. Chaudhari, A.K. Ghatge and S.A. Patil, 2000. Dielectric properties and electrical conduction of nickel ferrite-barium titanate composites. Indian J. Pure Applied Phys., 38: 615-620.
- Mori, K. and M. Wuttig, 2002. Magnetolectric coupling in terfenol-D/polyvinylidenedifluoride composites. Applied Phys. Lett., 81: 100-101.
- Nan, C.W., N. Cai, L. Liu, J. Zhai, Y. Ye and Y. Lin, 2003. Coupled magnetic-electric properties and critical behavior in multiferroic particulate composites. J. Applied Phys., 94: 5930-5936.
- Patankar, K.K., P.D. Dombale, V.L. Mathe, S.A. Patil and R.N. Patil, 2001. AC conductivity and magnetolectric effect in $MnFe_{1.8}Cr_{0.2}O_4$ -BaTiO₃ composites. Mater. Sci. Eng.: B, 87: 53-58.
- Rivera, J.P. and H. Schmid, 1991. Linear and quadratic magnetolectric (ME) effect in Ni-Cl boracite. J. Applied Phys., 70: 6410-6412.
- Sheikh, A.D. and V.L. Mathe, 2009. Effect of the piezomagnetic NiFe₂O₄ phase on the piezoelectric Pb (Mg_{1/3}Nb_{2/3})_{0.67}Ti_{0.33}O₃ phase in magnetolectric composites. Smart Mater. Struct., Vol. 18. 10.1088/0964-1726/18/6/065014.
- Suryanarayana, S.V., 1994. Magnetolectric interaction phenomena in materials. Bull. Mater. Sci., 17: 1259-1270.
- Van Den Boomgaard, J., A.M.J.G. Van Run and J.V. Suchtelen, 1976. Magnetolectricity in piezoelectric-magnetostrictive composites. Ferroelectrics, 10: 295-298.
- Van Run, A.M.J.G., D.R. Terrell and J.H. Scholing, 1974. An *in situ* grown eutectic magnetolectric composite material. J. Mater. Sci., 9: 1710-1714.
- Viswanathan, B. and V.R.K. Murthy, 1990. Ferrite Materials: Science and Technology. Narosa Publishing House, Mumbai, India, ISBN-13: 9780387529301, Pages: 198.
- Zhao, K., K. Chen, Y.R. Dai, J.G. Wan and J.S. Zhu, 2005. Effect of martensitic transformation on magnetolectric properties of Ni₂MnGa/PbZr_{0.52}Ti_{0.48}O₃ composite. Applied Phys. Lett., Vol. 87. 10.1063/1.2099545.